# Short-term forecasts and scaling of intense events in turbulence

**Diego A. Donzis** [*], **K.R. Sreenivasan** [* †]

[*] Institute for Physical Science and Technology, University of Maryland, College Park, MD, and [†] International Centre for Theoretical Physics, Trieste, Italy

Submitted to Proceedings of the National Academy of Sciences of the United States of America

**Large fluctuations in complex systems from earthquakes to financial markets, though infrequent, are particularly important because of their disproportionate impact. Our ability to forecast them is quite poor at present. Large fluctuations occur also in intermittent features of turbulent flows. Some dynamical understanding of these features is possible because the governing equations are known and can be solved exactly on a computer. Here we particularly study large-amplitude events of turbulent vorticity using results from direct numerical simulations of isotropic turbulence in conjunction with the vorticity evolution equation. We show that the advection of vorticity is the dominant process by which an observer fixed to the laboratory frame perceives it, and that the growth of squared-vorticity during large excursions is quadratic in time when normalized appropriately. This result is consistent with the multifractal description but simpler for present purposes. Computational data show that the peak in the viscous contribution can act as the precursor for the upcoming peak in vorticity, forming a reasonable basis for forecasts on short timescales that can be estimated simply. This idea might apply more broadly to forecasting other extreme quantities, e.g., in seismology.**

forecasting | extreme events | turbulent vorticity

Large earthquakes, huge floods, intense tornadoes and hurricanes, big crashes in stock-market values, and a number of other extreme events, have much larger impact than might be reckoned by the relatively low frequency of their occurrence. Forecasting such events is of obvious interest but of momentous challenge. By a forecast, we mean here the advance knowledge that a certain large event will occur with high probability within a known timescale following a suitable precursor. If successful predictions are possible in one complex system, something useful may be learnt about others as well.

Turbulence at high Reynolds numbers is replete with strong fluctuations in vorticity, dissipation and other features characteristic of small-scale motion. Extreme fluctuations of dissipation and vorticity can be hundreds or thousands of times the mean value [1, 2]. It is technically important to understand these extremes because of their relevance to reacting flows [3] and dispersion problems [4]; they are also objects of intense mathematical inquiry [5] and the center of attention in intermittency theories [6, 7]. Our interest here is to explore empirically the extent to which an isolated extreme event in turbulence can be predicted dynamically through a precursor. Such predictions are indeed difficult but we have here the luxury of well-posed differential equations governing the motion of turbulence. Though the equations are hard to understand analytically, it is reasonable to expect some success through their exact numerical solutions. This is the thrust of the paper.

The numerical database for our work comes from the exact or direct numerical simulation (DNS) of isotropic turbulence. We have performed three such simulations at Taylor microscale Reynolds numbers of 140, 240 and 400 to obtain all the terms in the vorticity equation [2]. We use the data to study the processes that dominate the time variation of vorticity at a fixed location, and identify precursors of extreme events. We find that advection dominates the dynamics for short times, and that the Eulerian growth of extreme vorticity follows a universal power-law with a single exponent when normalized by the proper timescale. Strong viscous activity typically precedes intense vorticity, and the advance time is given by a suitable combination of viscosity and large-scale velocity. In particular, the knowledge of the signs of the advective term and the vorticity determines in advance the occurrence of a local extremum in the latter.

The rest of the paper is organized as follows. We first describe the numerical simulations and the basic parameters that they employ. The dynamics of large fluctuations of vorticity are studied in the next section through the evolution equation. The timescales associated with large events are discussed and precursors of large fluctuations are presented. Finally, a summary and further outlook are offered.

## Numerical method and simulation parameters

Our interest is in the time evolution of vorticity $\omega_i$, whose governing equation

$$\partial\omega_i/\partial t = -u_j\omega_{i,j} + \omega_j u_{i,j} + \nu\omega_{i,jj}, \qquad [1]$$

is derived by taking the curl of the Navier-Stokes equations for an incompressible fluid. Here, $u_i$ represents the velocity components and $\nu$ is the kinematic viscosity of the fluid. The equations are solved using a massively parallel implementation of the pseudo-spectral method of [8]. Aliasing control by a combination of truncation and phase shifting methods is applied to compute all the terms in this equation, which implies double evaluations for the first two terms on the right. This adds a significant overhead to computational time. However, since we are interested in large fluctuations which take place on short

**Table 1. Basic parameters of the simulations: Taylor Reynolds number $R_\lambda$, grid resolution $N$, and different timescale ratios at the beginning of the simulation (denoted by the subscript $0$). $T_{E,0} = L/u_0'$ is the eddy-turnover time ($L$ being the large scale of turbulence and $u_0'$ the root-mean-square velocity), $\langle\tau_\eta\rangle_0 = (\nu/\langle\epsilon\rangle_0)^{1/2}$ is the Kolmogorov time scale, and $\langle\tau_v\rangle_0 = \nu/u_0'^2$ is a characteristic timescale of extreme events (see text). $\langle.\rangle$ indicates long-time average.**

| $R_\lambda$ | 140 | 240 | 400 |
|---|---|---|---|
| $N$ | 256 | 512 | 1024 |
| $T_{E,0}/\langle\tau_\eta\rangle_0$ | 14.5 | 23.7 | 40.8 |
| $T_{E,0}/\langle\tau_v\rangle_0$ | 459 | 1310 | 4244 |
| $\langle\tau_\eta\rangle_0/\langle\tau_v\rangle_0$ | 32 | 55 | 104 |

timescales, long simulations are not needed. In order to obtain a large number of samples, we compute the terms on the right hand side of equation **[1]** and store them at a number of locations in physical space at every time step. Homogeneity assures that specific locations are unimportant, and we choose them to be sufficiently distant from one another so that they are effectively independent.

The initial conditions are taken from stationary forced isotropic turbulence at the Reynolds numbers given in Table 1 and the resolution is such that the condition $k_{max}\eta \approx 1.5$ holds (where $k_{max}$ is the highest resolvable wavenumber and $\eta$ is the Kolmogorov scale representing nominally the smallest scale of dissipation). The simulations were continued without forcing. Since the simulation time was short, the final value of turbulent kinetic energy was always greater than half its initial value and the variation of the smallest timescale $\tau_\eta$ was less than 40%.

The time step was controlled by a constant Courant number of about $0.3$ which is smaller than in common practice [9]. This required the use of a time step that is two orders of magnitude smaller than the mean Kolmogorov timescale. Indeed, as we shall see subsequently, capturing the strongest events requires such a fine resolution.

## Dynamics of large fluctuations

**Power-law behavior and timescales.** To discuss the dynamics of large excursions in vorticity $\omega_i$, it is convenient to rewrite equation **[1]** as

$$\partial\omega_i/\partial t = -\mathcal{C}_i + \mathcal{W}_i + \mathcal{V}_i, \qquad \textbf{[2]}$$

where

$$\mathcal{C}_i = u_j\omega_{i,j}, \quad \mathcal{W}_i = \omega_j u_{i,j} \quad \text{and} \quad \mathcal{V}_i = \nu\omega_{i,jj}, \qquad \textbf{[3]}$$

representing the advective, vortex-stretching and viscous contributions, respectively. In Figure 1 we show a typical time series, for $\omega_1$, of all the terms in equation **[2]**. The figure shows that the advective term $\mathcal{C}_i$ accounts for much of the variation of $\omega_i$, especially when the vorticity amplitudes are large. The Eulerian picture is that large excursions of vorticity, perhaps related to vortical structures, are advected by the local flow past the measuring location. This observation, which

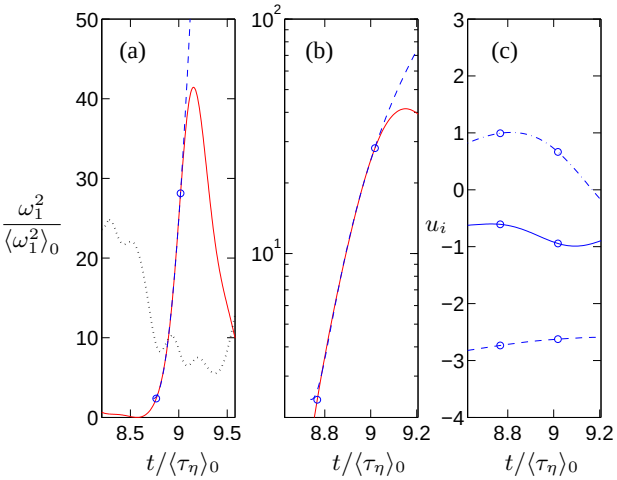


**Fig. 2.** Detailed view of a typical intense event at $R_\lambda \approx 400$. (a) Squared vorticity normalized by its space average at the beginning of the simulation. Dotted line corresponds to $10\epsilon/\langle\epsilon\rangle_0$ at the same location (the factor 10 has been used for clarity). (b) Squared vorticity on semi-log scale. (c) Velocity components during the time interval. Times are normalized by the initial space-averaged Kolmogorov time scale $\langle\tau_\eta\rangle_0$. Circles delimit the fitting range.

is consistent with the qualitative suggestions in [10] and [11], would imply that

$$\partial\omega_i/\partial t \approx -\mathcal{C}_i \qquad \textbf{[4]}$$

can approximate the dynamics of large fluctuations of vorticity. Vortex-stretching, which is the main mechanism for generating vorticity, makes a secondary contribution to the instantaneous balance of large fluctuations observed in Figure 1. Indeed, the physical picture is that large vorticity is generated on a longer timescale dictated mostly by vortex stretching and that, once created, it is advected by the flow on shorter time scales; let us denote the instantaneous advection velocity by $v$. Since viscous effects eventually prevent large spatial

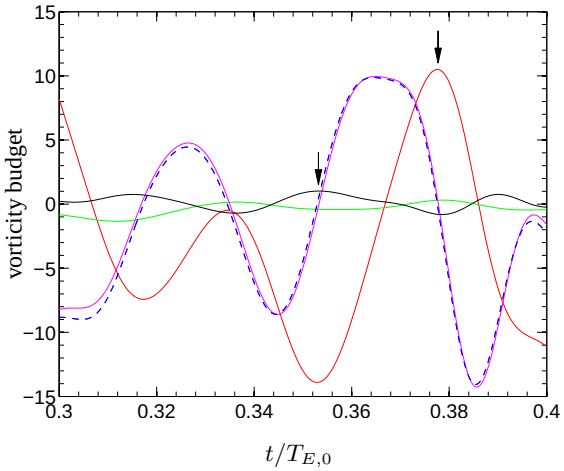


**Fig. 1.** Typical time series for the vorticity budget equation **[2]** at an arbitrary location for $R_\lambda \approx 240$. All quantities are normalized by the rms value of $\omega_1$ at $t = 0$ and by the initial eddy turnover time $T_{E,0} = L/u_0'$. Lines correspond to $\partial\omega_1/\partial t$ (dashed blue), $-\mathcal{C}_1$ (magenta), $\mathcal{W}_1$ (green) and $\mathcal{V}_1$ (black). The red line is $\omega_1$ multiplied by 10 for clarity.

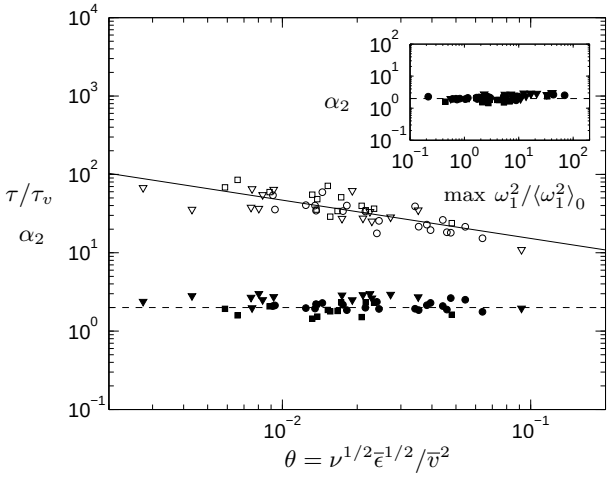


**Fig. 3.** The exponent $\alpha_2$ in equation **[6]** (filled symbols). Dashed line at 2 is for comparison. Normalized time scale $\tau/\tau_v$ in equation **[5]** (unfilled symbols). Circles, squares and triangles correspond to data at $R_\lambda \approx 140$, 240 and 400, respectively. Solid line is for $\tau/\tau_v \sim \theta^{-0.49}$. Inset: the exponent $\alpha_2$ as a function of the peak value of the corresponding large event.

gradients from forming, it is natural to think that both $\nu$ and $v$ will be the key variables for scaling the dynamics of large fluctuations.

Let us choose a particular spike. Since $\mathcal{C}_i$ dominates the right-hand-side of equation **[2]**, $\omega_i$ will have an inflection point at time $t'$ where the advection term has a local maximum. One can expand the solution around $t'$ which, to first order, is $\partial\omega_i/\partial t \approx c$ where $c$ is a constant (the local maximum of $\mathcal{C}_i$) taken as $1/\tau^2$ for convenience. Integration yields $\omega_i \approx {\omega_i}^0 + (t-t_0)/\tau^2$ where ${\omega_i}^0$ is the vorticity at $t_0$, typically much smaller than the peak value. Therefore, one expects

$$ {\omega_i}^2 \sim (t-t_0)^2/\tau^4 \qquad \textbf{[5]} $$

during those intervals in which vorticity grows fast. The quality of this prediction is shown in Figure 2 for a typical intense event at $R_\lambda \approx 400$. Equation **[5]** is seen to represent the data quite well for a range of fluctuations of more than an order of magnitude; this is so for all large peaks.

In the multifractal formalism, different magnitudes of squared-vorticity have different exponents [1], but equation **[5]** and the data presented here yield an exponent of 2 for all large magnitudes. The two views are, in fact, consistent if we note that $\tau$ in **[5]** depends on the intensity of each peak. A fuller discussion of this point is given in the Appendix.

To test **[5]** further, we have obtained least-square fits of the expression

$$ {\omega_i}^2 = [\alpha_1 (t-t_0)]^{\alpha_2} \qquad \textbf{[6]} $$

to intense events at different Reynolds numbers. The resulting $\alpha_2$ values are plotted in Figure 3 against the parameter $\theta = (\nu\overline{\epsilon})^{1/2}/\overline{v}^2$, with the overbar denoting the average over the duration of the peak vorticity. To be specific, we have used the averaging time to be the interval between the circles in Figure 2, but plausible variants do not affect the results significantly. The origin and interpretation of this parameter will be discussed momentarily. The inset of Figure 3 plots the same exponent $\alpha_2$ as a function of the maximum value of vorticity attained in each intense event examined. It appears that $\alpha_2 \approx 2$ holds for fluctuations of all intensities (which span almost three decades here, see inset) and for all $R_\lambda$.

The similarity scaling of $\tau$ is also shown in Figure 3. To understand this scaling, recall our earlier remark that $\nu$ and the advection velocity $v$ are our relevant parameters. We now note that $c = -u_j\omega_{i,j}$ (see equation **[4]**) and that $\varepsilon_{ijk}u_i\omega_{k,j} = \epsilon/\nu - 2(u_i s_{ij})_{,j}$, where $\varepsilon_{ijk}$ is the alternating tensor and $\epsilon$ is the energy dissipation rate. The last expression shows that cross-terms involving components of velocity and vorticity gradients are related in part to instantaneous dissipation kinematically. Moreover, it has been consistently found that intense enstrophy events are *preceded* by intense dissipation events [10, 11]. Therefore, in view of equation **[4]**, it is reasonable to assume that $\epsilon$ is also a key parameter in determining the dynamics close to an intense vortical event. On dimensional grounds, $\nu$, $\overline{v}$ and $\overline{\epsilon}$ can be combined to form two timescales $\tau_v = \nu/\overline{v}^2$ and $\tau_\eta = (\nu/\overline{\epsilon})^{1/2}$ and a non-dimensional parameter $\theta = \sqrt{\nu\overline{\epsilon}}/\overline{v}^2$. To get an appreciation for the order of magnitude of $\tau_v$, we list in Table 1 its *global* average value, $\langle . \rangle$, by replacing $\overline{v}^2$ by the global mean-square velocity ${u'}^2$. Incidentally, one can show that $\langle\tau_v\rangle/\langle\tau_\eta\rangle \sim {R_\lambda}^{-1}$ which suggests that a more stringent time resolution than the classical $-3/4$ power is required for high-$R_\lambda$ simulations and experiments [7].

In Figure 2, it is clear that even when the vorticity varies by orders of magnitude, the velocity remains approximately constant (part (c) of the figure). This is consistent with the well-known fact that vorticity and velocity gradients vary on shorter time scales than the velocity itself. On the other hand, the variation of the dissipation over the same interval is substantial as can be seen in Figure 2(a). Dimensional analysis yields

$$ \tau = \tau_v f(\theta) \qquad \textbf{[7]} $$

where $\theta = \nu^{1/2}\overline{\epsilon}^{1/2}/\overline{v}^2$ and $f$ is some universal function. The DNS results at different Reynolds numbers are included in Figure 3 (open symbols). In spite of some scatter, the data in Figure 3 support the scaling suggested by equation **[7]**, and can be fitted to the expression $\tau/\tau_v \sim \theta^{-\gamma_\theta}$ with $\gamma_\theta \approx 0.49$. We have convinced ourselves that the results do not change qualitatively if $\theta$ and $\tau$ are defined through other plausible averaging times.

Each intense event is slightly different since equation **[4]** is only an approximation that depends on the relative weights of advection, vortex-stretching and dissipation; the levels of $\mathcal{W}_i$ and $\mathcal{V}_i$ would, in fact, be different in the neighborhood of different spikes giving somewhat different values of the constant $c$. Nevertheless, the DNS data follow the simple correlation with constant $\alpha_2$. In principle, it would be possible to account for fluctuations of $\mathcal{W}_i$ and $\mathcal{V}_i$ as random variables on the right-hand-side of equation **[4]**, which could lead to an additive noise to $\tau$ in equation **[7]**. The distribution of $\tau$ may be related to the scatter in Figure 3, and its statistical properties should then be expressible in terms of vortex-stretching and viscous contributions. This effect, however, would weaken with increasing Reynolds numbers because the intense events and advection effects would both become stronger.

We emphasize that the scaling ${\omega_i}^2 \sim t^2$ is simply a first order expansion around the local maximum of $\partial\omega_i/\partial t$. This general observation applies to any function. What is particular to turbulence is that the timescale associated with this growth can be related to a simple combination of parameters. This is mainly because a single process dominates the right-hand-side of equation **[2]**. If, for instance, advection grows in time but viscous terms attain large negative values to balance advection, the proper timescale for the growth of $\omega_i$ will have a more complex scaling.

A further point is in order. From equation **[7]** it may appear that intense vorticity events are completely determined by local conditions. This raises questions on the global organization observed in turbulent flows. Our derivations for the behavior of $\omega_i$ contain the velocity $\mathbf{u}$ and the dissipation rate $\epsilon$. In terms of vorticity, the velocity field can be written as $\mathbf{u}(\mathbf{x}) = -1/4\pi \int_\Lambda \boldsymbol{\omega}(\mathbf{x}-\mathbf{r}) \times \mathbf{r}/|\mathbf{r}|^3 d^3\mathbf{r}$, where $\Lambda$ is the periodic domain. This equation makes it clear that the velocity at a particular location contains information from vorticity everywhere, especially from a neighborhood of $\mathbf{x}$ (due to the factor $\mathbf{r}/|\mathbf{r}|^3$). A similar integral relation can be obtained for velocity gradients and thus for $\epsilon$ (see, e.g., [12]). Therefore, equations **[5]** and **[7]** do not mean that only local information is adequate to address the scaling of intense vortical events.

**Precursors of large fluctuations.** The results in the previous section show that large fluctuations are approximated well by equation **[4]**. Therefore, large values of $\mathcal{C}_i$ lead to large time derivatives which will result in a $t^2$ growth of squared vorticity. Of course, due to the integral relation between $\mathcal{C}_i$ and $\omega_i$, there will be a time lag between a large value of advective terms and a peak in $\omega_i$. This is clearly seen in Figure 1 where large $\omega_i$ (red line) appears later than a large value of $\mathcal{C}_i$ (magenta line). Furthermore, large advective terms are preceded by local maxima of viscous terms (black line in the figure). This feature can be understood if one writes the viscous term as $\mathcal{V}_i = \nu(\partial/\partial x_j)(\partial\omega_i/\partial x_j)$ and replaces $\partial/\partial x_j$ by $(1/\overline{v})\partial/\partial t$. This leads to $\mathcal{V}_i \approx (\nu/\overline{v})(\partial/\partial t)(\partial\omega_i/\partial x_j)$ which, to a first approximation, can be written from definitions **[3]** as $\partial\omega_i/\partial x_j \approx \mathcal{C}_i/\overline{v}$ within

the short interval where vorticity peaks, so that

$$\frac{\partial \mathcal{C}_i}{\partial t} \approx \frac{1}{\tau_v}\mathcal{V}_i, \qquad \textbf{[8]}$$

showing that $\tau_v$ is a natural timescale of the problem. Indeed, if one assumes that $\mathcal{V}_i$ is represented by a single Fourier mode with frequency $\varpi$ and amplitude $\hat{\mathcal{V}}_i$, equations **[4]** and **[8]** suggest that $\mathcal{V}_i$ arrives earlier than $\omega_i$ by the time interval of $2\pi\tau_v/\varpi$. In other words, the time interval $\Delta t^*$ between the local maxima for $\mathcal{V}_i$ and $\omega_i$ (illustrated in Figure 1 as the interval between the arrows on the curves for $\omega_1$ and $\mathcal{V}_1$), is of the form

$$\Delta t^* \sim \tau_v. \qquad \textbf{[9]}$$

We automate the search for scaling of equation **[9]** by first focusing attention on values of $\omega_1^2$ greater than, say, 30 times the mean-square value for the time series obtained at one spatial location. Then, for each such peak, a prior local maximum of $\mathcal{V}_i$ is identified within an interval of a few mean Kolmogorov time scales. Experience shows that the precise choice of this interval is not critical for the scaling to be determined. This simple approach, however, does miss some spikes: in the chosen interval, there may be more than one maximum for $\mathcal{V}_i$ or more than one $\omega_i$ above the specified threshold. The data presented here capture conditions properly for about 75% of the samples above the threshold. We are interested in the time between the local maxima for $\mathcal{V}_i$ and $\omega_i$, denoted here as $\Delta t^*$.

We now empirically verify equation **[9]** by measuring $\Delta t^*$ and $\tau_v$ independently. To capture the dynamics over the interval between local maxima of $\mathcal{V}_i$ and $\omega_i$, it is more convenient to average the velocity $v$ over the longer time $\Delta t^*$; the results to be discussed below are robust with respect to the use of this longer averaging time since, as seen in Figure 2, the velocity varies significantly only over an even longer time. In Figure 4 we see that the data for $R_\lambda \approx 140$, 240 and 400 follow

$$\Delta t^* \approx 24\tau_v^{0.93}, \qquad \textbf{[10]}$$

which is only slightly different from equation **[9]**. The agreement in Figure 4 is good especially because this scaling is not of statistical nature but corresponds to individual trajectories in phase space. It is also the case that the present argument lacks the connection to geometrical aspects of the vectors and tensors involved. In particular, the model does not consider the effect of alignments between the velocity vector $\mathbf{u}$ and the gradient $\nabla\omega_1$ which make up the advective term (i.e. $\mathcal{C}_1 = \mathbf{u}\cdot\nabla\omega_1 = |\mathbf{u}||\nabla\omega_1|\cos(\mathbf{u}, \nabla\omega_1)$). These aspects can be taken into account at the next level of refinement, presumably reducing the scatter in Figure 4. Finally, as stressed in previous sections, equation **[4]** contains in reality some contribution from $\mathcal{V}_i$ and $\mathcal{W}_i$, which may be different for each intense event. In this sense, the scaling **[9]** can be regarded as an average result.

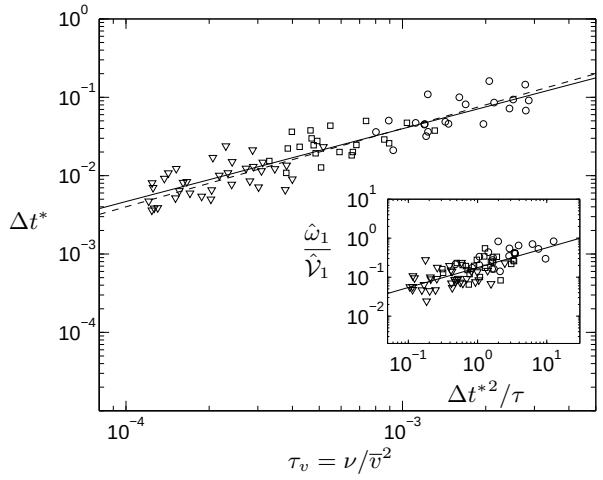


**Fig. 4.** The time interval $\Delta t^*$ between the arrivals of a peak in viscous terms and the subsequent peak in vorticity plotted against the time scale $\tau_v$ for $R_\lambda \approx 140$ (◯), 240 (□) and 400 (▽). Dashed line: slope 1. Solid line: equation **[10]** which is the best fit to the data. Inset: scaling of the ratio of local maxima for vorticity $\hat{\omega}_1$ and viscous terms $\hat{\mathcal{V}}_1$.

To get some idea of the relation between the amplitude of $\omega_i$ and $\mathcal{V}_i$, we may again resort to a single Fourier component for the viscous term with amplitude $\hat{\mathcal{V}}_i$. Equations **[4]** and **[8]** then imply $\hat{\omega}_1/\hat{\mathcal{V}}_1 \sim \tau_v/\varpi^2$. Now, we use the previous result $\Delta t^* \sim \tau_v/\varpi$ to find that the amplitude ratio scales as $\hat{\omega}_1/\hat{\mathcal{V}}_1 \sim \Delta t^{*2}/\tau_v$. To compare this prediction with the DNS results, the vorticity "amplitude" is taken as the difference between the maximum value and that at the time $\mathcal{V}_i$ peaks; this difference measures the actual growth. The results are shown in Figure 4 (inset) where the data follow the power-law trend although the slope is smaller than the expected value of unity (0.53 from the best fit). This result as well as the greater scatter than in the main frame in Figure 4 are not unexpected because, although $\tau_v$ is the natural timescale for the problem, the dimensional scaling for the ratio of amplitudes relies on $\mathcal{V}_i$ behaving as a single sinusoid.

The scaling of equation **[9]** shown in Figure 4 was obtained by analyzing time series backwards: how far back in time with respect to an intense vorticity event does a local extremum in $\mathcal{V}_i$ occur? We can now ask the more important question of forecast: how long after observing a local maximum in the viscous event does it take for intense vorticity to build up to its peak value? We first note that large $\mathcal{C}_i$ will not always lead to large $\omega_i$. An example is seen in Figure 1 at $t/T_{E,0} \approx 0.326$ where $\mathcal{C}_i$ attains a large value but $\omega_i$ is negative for a long interval of time. Thus, the large positive time derivative is not enough by itself to make $\omega_i$ grow to large positive values.

We now proceed to explain the last statement better. First, we find the local maximum (or minimum) in $\mathcal{V}_i$ if it is positive (or negative). Since we are primarily interested in large fluctuations, we simultaneously set a threshold on $\mathcal{V}_i$. Let us denote a qualified maximum (or minimum) by $\hat{\mathcal{V}}_i$ and the time at which it occurs by $t_{\hat{\mathcal{V}}_i}$, and let the total number of such viscous events, both positive and negative, observed for a given Reynolds number be $N_{\hat{\mathcal{V}}_i}$. We now look for a local extremum for $\omega_i$ in an interval of time given by $c \times 24\tau^{0.93}$ (see equation **[10]**) where the prefactor $c = 2$ roughly accounts for the scatter observed in Figure 4. If a local extremum exists, we increment $N_{\hat{\omega}_i}$, the total number of extrema for $\omega_i$ following an intense viscous

**Table 2. Intense viscous event as a precursor for the subsequent large vorticity event. The threshold for $\mathcal{V}_i$ is $\langle\omega_1^2\rangle_0$. See text for explanations of different quantities.**

| $R_\lambda$ | 140 | 240 | 400 |
|---|---|---|---|
| $N_{\hat{\mathcal{V}}_i}$ | 190 | 198 | 155 |
| $P(\hat{\omega}_i\|\hat{\mathcal{V}}_i)$ | 0.71 | 0.71 | 0.72 |
| $P(\text{sign}(\hat{\omega}_i) = \text{sign}(\hat{\mathcal{V}}_i)\|\hat{\mathcal{V}}_i)$ | 0.48 | 0.45 | 0.50 |
| $P(\text{sign}(\hat{\omega}_i) = \text{sign}(\hat{\mathcal{V}}_i)\|\hat{\mathcal{V}}_i, (++/--))$ | 1.00 | 1.00 | 1.00 |
| $P(\text{sign}(\hat{\omega}_i) = \text{sign}(\hat{\mathcal{V}}_i)\|\hat{\mathcal{V}}_i, (+-/-+-))$ | 0.82 | 1.00 | 0.77 |
| $P(\text{sign}(\hat{\omega}_i) = \text{sign}(\hat{\mathcal{V}}_i)\|\hat{\mathcal{V}}_i, (++-/--+))$ | 0.88 | 0.78 | 0.80 |

event. In Table 2 we show $N_{\hat{\mathcal{V}}_i}$ and $P(\hat{\omega}_i|\hat{\mathcal{V}}_i)$, the probability of finding a local extremum of $\omega_i$ knowing that there was an intense viscous event (i.e. the ratio $N_{\hat{\omega}_i}/N_{\hat{\mathcal{V}}_i}$), for different Reynolds numbers using a threshold for $\mathcal{V}_i$ equal to $\langle\omega_1^2\rangle_0$. The Table (third row) shows that slightly more than 70% of intense viscous events are followed by the maxima in vorticity in the interval given by equation **[10]** for all $R_\lambda$. Note that this result comprises of local extrema for $\omega_i$ of both signs. On the other hand, the probability with which a positive (negative) sign of large $\mathcal{V}_i$ would lead to a large positive (negative) sign of $\omega_i$ is close to 50% (fourth row of Table 2)—an essentially random connection.

It is possible to use additional information about the state of the system at $t_{\hat{\mathcal{V}}_i}$ to predict more accurately when a strong vorticity event will succeed a strong viscosity event. To do this, we distinguish different cases based on the signs of $\mathcal{V}_i$, $-\mathcal{C}_i$ and $\omega_i$ at $t = t_{\hat{\mathcal{V}}_i}$. A state of the system will be denoted by $(+\,+\,+)$ if $\text{sign}(\mathcal{V}_i(t_{\hat{\mathcal{V}}_i})) = 1$, $\text{sign}(-\mathcal{C}_i(t_{\hat{\mathcal{V}}_i})) = 1$ and $\text{sign}(\omega_i(t_{\hat{\mathcal{V}}_i})) = 1$ or $(+\,-\,-)$ if $\text{sign}(\mathcal{V}_i(t_{\hat{\mathcal{V}}_i})) = 1$, $\text{sign}(-\mathcal{C}_i(t_{\hat{\mathcal{V}}_i})) = -1$ and $\text{sign}(\omega_i(t_{\hat{\mathcal{V}}_i})) = -1$. Now we look at the probability of finding an extreme $\hat{\omega}_i$ given that there was an intense viscous event $\hat{\mathcal{V}}_i$, and that the configuration is given by $(+\,+\,+)$. Other combinations can be defined similarly. Note that $(+\,+\,+)$ and $(-\,-\,-)$ are equivalent, as are $(+\,-\,+)$ and $(-\,+\,-)$. The equivalent states are also collected together in Table 2. We see that, when $\mathcal{V}_i$, $-\mathcal{C}_i$ and $\omega_i$ all have the same sign (i.e., $(+\,+\,+$ or $-\,-\,-)$), an intense viscous event always results in a local extremum for $\omega_i$ of the same sign, with the intensity that may be related to the scaling shown in the inset of Figure 4. If either $-\mathcal{C}_i(t_{\hat{\mathcal{V}}_i})$ or $\omega_i(t_{\hat{\mathcal{V}}_i})$ has a different sign, the probability is reduced as expected—to about 80% at all Reynolds numbers.

Thus, we find that the viscous term $\mathcal{V}_i$ is a reasonable precursor for intense vorticity events on timescales of the order of $\tau_v$. If this information is supplemented by the sign of the advective term and vorticity itself at the instant $\mathcal{V}_i$ peaks, the precursor becomes more definitive. Although the conditional probabilities shown in Table 2 appear to be independent of the Reynolds number, longer time series and a wider range of Reynolds numbers are needed to strengthen this assertion.

## Discussion and conclusions

We have shown that large viscous contributions anticipate the arrival of large vorticity events. This statement can be understood as follows. Since advection dominates, gradients in space and time are related by a velocity. Therefore, gradients of vorticity gradients (i.e., viscous terms) may be treated as time derivatives of vorticity gradients and therefore may "announce" large vorticity gradients or, for quasi-constant velocity, large advective terms. The structure of the fluid dynamic equations makes viscous terms (under the dominance of advection) "look like" the second time derivative of vorticity and is capable of anticipating the arrival of large vorticity. This anticipation cannot be expected to hold true for a long period.

All intermittent quantities of turbulence (such as squared vorticity and dissipation) are governed by equations with similar structure to equation **[2]**, with the "sources" $\mathcal{W}_i$ and $\mathcal{V}_i$ replaced suitably. Whenever the contributions from all these processes are small compared to $\mathcal{C}_i$ for intense events, equation **[4]** applies qualitatively. Therefore, it is possible that the scaling laws proposed here may hold for all intermittent quantities. The physical picture would be that they would all be advected by the flow on short timescales but different processes would be responsible for building up large fluctuations on longer time scales.

Although we do not have the luxury of well-tested differential equations for many extreme events occurring in nature, we believe that knowledge from turbulence could prove valuable for them as well. It has already been observed in [2] and theorized in [13, 14, 15] that some universal behavior may govern all extreme phenomena. In seismology, for instance, there is some evidence for the existence of precursory motion for earthquakes and after-shocks; see, for example, [22]. In particular, measured displacement shows departures from long-term trends which will first be captured by changes in second time-derivatives. It is conceivable that this precursor is related to some kind of dissipation. Even for non-Newtonian fluids, viscous contributions are determined by velocity gradients, so strong viscous terms may serve as a precursor for intense events if space and time can be related (as shown to be the case for vorticity events). A more rigorous relation between fault dynamics and fluid mechanics is part of our ongoing research.

While our results do not depend qualitatively on averaging times and procedures, there are at least two limitations to our proposal on precursors. First, the timescale over which "predictions" are possible is relatively short; it is unclear if forecasts over longer times would be possible in practice. Second, it is not obvious that one can measure the second derivative of the signal with adequate accuracy. It presents no problem in a clean system such as computational turbulence but, in general, one has to apply some filtering to the signal without losing its substance. Work relating to such questions are also the subject of a continuing study.

## Appendix

Here, we explore the connection between the present model of large fluctuations with other descriptions in the literature. Since equation **[5]** represents large fluctuations one would expect that a model based on this functional form should be able to reproduce high-order statistics from experimental and numerical data as well as the widely used multifractal (MF) models [7]. One can use a collection of power-law events of the form

$$\tilde{\omega}_1^2(t) \approx \begin{cases} [(t-t_{0-})/\tilde{\tau}]^\beta/\tilde{\tau}^2 & t_{0-} \le t < t_p \\ [(t_{0+}-t)/\tilde{\tau}]^\beta/\tilde{\tau}^2 & t_p \le t < t_{0+} \end{cases} \qquad \textbf{[11]}$$

and zero otherwise, where $t_p$ is the time at which $\tilde{\omega}_1^2$ attains its maximum, $a$, $t_{0\pm} = t_p \pm \delta t$, and $\delta t = \tilde{\tau}(\tilde{\tau}^2 a)^{1/\beta}$ so that $\omega_1^2(t_p) = a$. In

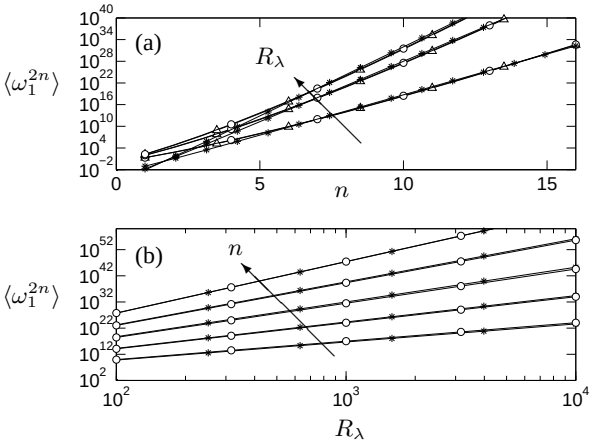


**Fig. 5.** Scaling of moments according to MF [16] (◯), the theory of [7] (△) and equation **[12]** with effective parameters $a^*$ and $\tilde{\tau}$ (∗). (a) Curves are for $R_\lambda = 100, 500$ and $1000$. (b) Even moments from $n = 6$ to $14$.

this case, one obtains moments that scale as

$$\langle \tilde{\omega}_1^{2n} \rangle \sim 2a^{1/\beta} \tilde{\tau}^{1+2/\beta} \frac{a^n}{1+\beta n}. \qquad \textbf{[12]}$$

We have tested this scaling for signals with a number of spikes with different amplitudes $a$ and times scales $\tilde{\tau}$ and found that **[12]** is quite accurate if one uses "effective" parameters $a^*$ and $\tilde{\tau}^*$ to fit the data. In Figure 5(a), we show moments of squared vorticity according to the MF formalism [16], the theory in [7] and equation **[12]** with parameters $a^*$ and $\tilde{\tau}^*$ chosen as best fit to the MF model for $n \geq 5$ at three Reynolds numbers in the range of our simulations. As with some other models ([19, 17]), it is virtually impossible to distinguish our model from the others from such comparisons alone. The matter is somewhat more obscure: by using "exponential" spikes defined by $ae^{c(t-t_p)}$ if $t \leq t_p$ and $ae^{-c(t-t_p)}$ if $t > t_p$, one obtains $\langle \tilde{\omega}_1^{2n} \rangle \sim a^n/(nc)$ which is the same scaling as **[12]** for large $n$. Because the MF model and both power-law (for any $\beta$) and exponential spikes all give the same scaling for high-order moments, the conclusion is that little can be said about the local structure of intense events from such global comparisons.

Nevertheless, it is of interest to explore the connection between the present and the MF models. The fundamental assumption behind the latter is that the total dissipation in a $d$-dimensional box of size $r$ scales as $E_r = \int_r \epsilon \, dr \sim r^{\alpha-1+d}$ (a similar quantity can be defined for $W_r = \int_r \omega^2 \, dr \sim r^{\alpha'-1+d}$). In Ref. [21] this scaling was tested for the dissipation surrogate $(\partial u/\partial t)^2$ by plotting $E_r$ as a function of $r$. Their data are reproduced here in Figure 6(b) along with the approximate power law (dashed line) suggested by those authors. In Figure 6(a), we show the scaling of the integral $(\tilde{W}_1)_t = \int_0^t \tilde{\omega}_1^2 dt$ where $\tilde{\omega}_1^2$ is composed of six spikes of the form of equation **[11]** with different $t_p$ and amplitudes $a$. Comparison of parts (a) and (b) reveals the same approximate power-law behavior. It is therefore not surprising that similar predictions are found for the scaling of moments.

Because $a^*$ is a measure of the strongest fluctuations, it is of interest to investigate its Reynolds number scaling. We found that the present model reproduces the MF predictions if one uses simple power laws $a^* \sim {R_\lambda}^{\gamma_a}$, $\tilde{\tau}^* \sim {R_\lambda}^{\gamma_\tau}$ and $M \sim {R_\lambda}^{\gamma_M}$ (where $M$ is the number of spikes) with $\gamma_a \approx 1.60$, $\gamma_\tau \approx -0.84$ and $\gamma_M \approx 1.75$. Using this result, we can determine the Reynolds number scaling of moments of different orders as

$$\langle \tilde{\omega}_1^{2n} \rangle \sim {R_\lambda}^{n\gamma_a + \rho - \log n/\log R_\lambda}, \qquad \textbf{[13]}$$

where $\rho = \gamma_a/\beta + \gamma_\tau(1+2/\beta) - \gamma_M$. This equation shows a logarithmic correction to a simple power law at finite Reynolds numbers.

Another way to recast the MF model is to use local averages: $\epsilon_r/\langle\epsilon\rangle \sim (r/L)^{\alpha-1}$ for energy dissipation or $\omega_r^2/\langle\omega^2\rangle \sim (r/L)^{\alpha'-1}$ for squared-vorticity. We are now interested in the the limit $r \to 0$, so that $r$ lies within an intense event. In the present model, we could write $\omega_r^2/\langle\omega^2\rangle \sim (r/r_\tau)^2$ (see equation **[5]**), where $r_\tau$ a suitably defined scale (e.g., $r_\tau \approx v\,\tau$, this being a function of time and space). This result suggests a simpler object if scales are normalized by $r_\tau$ instead of $L$. In fact, we could write, at each location, $r_\tau^2\omega_r^2 \sim \langle\omega^2\rangle r^2$ and compute moments to obtain $\langle (r_\tau^2\omega_r^2)^n \rangle \sim \langle\omega^2\rangle^n r^{2n}$ (for $r \to 0$). This result, which can also be applied to $\epsilon$, can be deduced from dimensional arguments on $r_\tau^2\epsilon_r$, for example, if the important parameters are $\langle\epsilon\rangle$ and $r$.

We appreciate helpful collaboration with P.K. Yeung on the simulations. This work was supported by the National Science Foundation Grant CTS-0553602 to the University of Maryland.

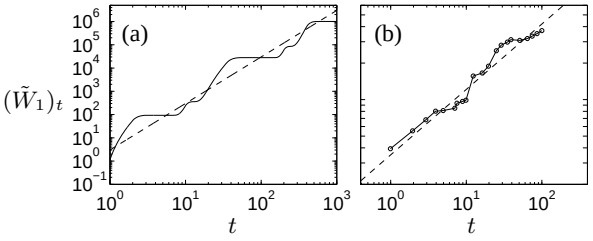


**Fig. 6.** (a) The integral $(\tilde{W}_1)_t = \int_0^t \tilde{\omega}_1^2 dt'$ for a signal composed of six spikes of the form equation **[11]**. Dashed line is a power-law for comparison. (b) Experimental data from [21] (figure 1c in their paper). Dashed line is the power-law fit from that reference. The two figures are in arbitrary units.


1. Sreenivasan, K.R., and Meneveau, C. (1988) Singularities of the equations of fluid motion. *Phys. Rev. A* **38** 6287-6295.
2. Donzis, D.A., Yeung, P.K., and Sreenivasan, K.R. (2008) Dissipation and enstrophy in isotropic turbulence: Resolution effects and scaling in direct numerical simulations. *Phys. Fluids* **20** 045108.
3. Sreenivasan, K.R. (2004) Possible effects of small-scale intermittency in turbulent reacting flows. *Flow Turb. Combust.* **72** 115-131.
4. Borgas, M.S., and Yeung, P.K. (2004) Relative dispersion in isotropic turbulence. Part 2. A new stochastic model with Reynolds-number dependence. *J. Fluid Mech.* **503** 125-160.
5. Gibbon, J.D., and Doering, C.R. (2005) Intermittency and regularity issues in 3D Navier-Stokes turbulence. *Arch. Rat. Mech. Anal.* **177** 115-150.
6. Frisch, U. (1995) Turbulence. Cambridge University Press, Cambridge.
7. Yakhot, V., and Sreenivasan, K.R. (2005) Anomalous scaling of structure functions and dynamic constraints on turbulence simulations. *J. Stat. Phys.* **121** 823-841.
8. Rogallo, R.S. (1981) Numerical experiments in homogeneous turbulence. *NASA Ames Research Center*, Moffett Field, CA. 81315.
9. Eswaran, V., and Pope, B.S. (1988) An examination of forcing in direct numerical simulations of turbulence. *Comput. Fluids* **16** 257-278.
10. Zeff, B.W., Lanterman, D.D., McAllister, R., Roy, R., Kostelich. E.J., and Lathrop, D.P. (2003) Measuring intense rotation and dissipation in turbulent flows. *Nature* **421** 146-149.
11. Lee, S., and Lee, C. (2005) Intermittency of acceleration in isotropic turbulence. *Phys. Rev. E.* **71** 056310.
12. Constantin, P. (1994) Geometric statistics in turbulence. *SIAM Review* **36** 73-98.
13. L'vov, V., and Procaccia, I. (1996) The universal scaling exponents of anisotropy in turbulence and their measurements. *Phys. Fluids* **8** 2565-2567.
14. Nelkin, M. (1999) Enstrophy and dissipation must have the same scaling exponents in the high Reynolds number limit of fluid turbulence. *Phys. Fluids* **11** 2202-2204.
15. He, G., Chen, S., Kraichnan, R.H., Zhang, R., and Zhou, Y. (1998) Statistics of Dissipation and Enstrophy Induced by Localized Vortices. *Phys. Rev. Lett.* **81** 4636-4639.
16. Nelkin, M. (1990) Multifractal scaling of velocity derivatives in turbulence. *Phys. Rev. A* **42** 7226-7229.
17. Schumacher, J., Sreenivasan, K.R., and Yakhot, V. (2007) Asymptotic exponents from low-Reynolds-number flows. *New. J. Phys.* **9** 89-108.
18. She, Z-S., and Leveque, E. (1994) Universal scaling laws in fully-developed turbulence. *Phys. Rev. Lett.* **72** 336-339.
19. Nelkin, M. (1995) Inertial range scaling of intense events in turbulence. *Phys. Rev. E* **52** R4610-R4611.
20. Sreenivasan, K.R., and Antonia, R.A. (1997) The phenomenology of small-scale turbulence. *Annu. Rev. Fluid Mech.* **29** 435-472.
21. Meneveau, C., and Sreenivasan, K.R. (1987) The multifractal spectrum of the dissipation field in turbulent flows. *Nucl. Phys. B* **2** 49-76.
22. Melbourne, T.I., and Webb, F.H. (2002) Precursory transient slip during the 2001 $M_w = 8.4$ Peru earthquake sequence from continuous GPS. *Geophys. Res. Lett.* **29** art. no. 2032.